Chaos
An Interdisciplinary Journal of Nonlinear Science

RESEARCH ARTICLE | SEPTEMBER 04 2025

Traffic flow-oriented reliability assessment and enhancement of urban transportation networks FREE

Yihong Bao ; Qihang Chen ; Dingding Han

Chaos 35, 093101 (2025)
https://doi.org/10.1063/5.0277379

Chaos ARTICLE pubs.aip.org/aip/cha

Traffic flow-oriented reliability assessment and enhancement of urban transportation networks

Cite as: Chaos 35, 093101 (2025); doi: 10.1063/5.0277379
Submitted: 23 April 2025 · Accepted: 5 August 2025 ·
Published Online: 4 September 2025

Yihong Bao, Qihang Chen, and Dingding Han[a)]

AFFILIATIONS

School of Information Science and Technology, Fudan University, Shanghai 200433, China

[a)]**Author to whom correspondence should be addressed:** ddhan@fudan.edu.cn

ABSTRACT

System reliability is a critical aspect of urban transport networks. It ensures that modern cities can provide safe, efficient, and resilient mobility services. However, existing reliability studies primarily focus on network topology and connectivity, overlooking the impact of disruptions on passenger travel quality and the temporal heterogeneity inherent in traffic patterns. Here, we propose a traffic flow-oriented reliability analysis method. This method integrates real-world passenger flow data into a percolation-based reliability evaluation. Specifically, we construct a weighted network model that accounts for commuting time costs and transfer penalties. We also introduce traffic-aware centralities to identify critical links and propose reliability metrics that consider both traffic flow preservation and travel time variation in the event of disruptions. We further evaluate two protection strategies to enhance system reliability. We apply our approach to the Shanghai metro system and conduct extensive numerical simulations across different traffic patterns. Our results show that failing to consider travel quality can lead to an underestimation of network vulnerability. We also demonstrate that a centrality-based protection strategy improves the effectiveness and repeatability of protected links under similar traffic patterns. This study offers a data-driven, temporally adaptive methodology for evaluating and enhancing the reliability of urban transportation systems, providing insights for infrastructure planning and risk management in smart cities.

Reliable urban transportation is essential for maintaining continuous service, particularly during disruptions. In demand-driven networks, where travel time and quality are crucial to user experience, service can degrade significantly even when connectivity is maintained. Furthermore, the temporal variability of traffic, which fluctuates across hours and days, is often neglected in traditional assessments, despite its considerable impact on performance. In light of these challenges, we propose a novel traffic flow-oriented reliability analysis method that accounts for both travel demand preservation and time-dependent service degradation under varying traffic patterns. We introduce traffic-aware centrality and reliability metrics for percolation-based functional assessments and evaluate two link protection strategies to enhance network reliability. This study offers valuable insights for smart infrastructure planning and reliability management in urban transportation systems.

I. INTRODUCTION

Urban transportation networks form the backbone of modern cities by providing high-capacity, efficient, and sustainable mobility solutions. As these networks grow in scale and complexity, ensuring their operational reliability becomes increasingly critical. The reliability of urban transportation networks directly influences the overall system performance, service continuity, and passenger satisfaction, particularly under disruptions or unexpected failures. Viewing transportation infrastructure through the lens of networks enables a deeper understanding of system vulnerabilities.[1–5] By leveraging the theoretical foundations and computational techniques of network science, researchers can rigorously quantify system functionality under various perturbations, supporting the development of more resilient and efficient urban mobility systems.[6]

Transportation systems are often vulnerable to disruptions, making their reliability a critical concern. In the field of complex

networks,[7–12] percolation theory is widely applied to assess the reliability and resilience of networked systems by simulating the progressive removal of nodes or links according to specific attack strategies.[13–23] By analyzing how the network decomposes and undergoes phase transitions during these perturbations, percolation theory provides insights into the structural and functional maintenance of the network system.[6] Reliability and resilience are two closely related but distinct concepts in the study of system functionality maintenance.[24] Reliability refers to a network's ability to maintain its core structure and functionality despite disruptions,[25] whereas resilience is a broader, multi-faceted concept encompassing an infrastructure's capacity to anticipate, absorb, recover from, and adapt to adverse events over its lifecycle.[26,27] Unlike resilience, which includes post-disruption recovery, this study focuses on analyzing the network's ability to maintain performance under disruptions, emphasizing pre-disruption assessment and prevention.

Many studies on network reliability focus on variations in giant component sizes or topological connectivity during percolation processes, which assess structural reliability.[28] However, transportation networks are demand-driven service networks where connections are shaped by social behavior and mobility needs between node pairs.[29] In such systems, links carrying higher volumes of traffic often reflect a collective travel pattern and tend to be more critical.[30] In demand-driven networks, even if large components collapse, the overall network performance can still be maintained at a satisfactory level if most traffic demands are concentrated within smaller connected components during the percolation process.[31] Therefore, it is crucial to consider network functionality in the reliability assessment of urban transportation systems. Several recent studies have explored traffic-aware network approaches to assess the functionality of transportation systems, but some practical traffic factors may still be underrepresented. For instance, Xu and Chopra[32] proposed a spatial–temporal resilience cycle framework that evaluates metro system performance across stages. While their method incorporates temporal traffic flows, it primarily emphasizes travel connectivity and recovery speed, with limited attention to passenger rerouting behavior or real-time performance degradation. Lordan and Sallan[33] introduced dynamic network measures that account for varying shortest paths and temporal centrality. However, their approach lacks real passenger demand data and does not assess reliability under disruptions. Hamedmoghadam *et al.*[31] introduced a percolation-based model incorporating heterogeneous flow demand to identify structural bottlenecks. Their analysis is based on static link quality assumptions and binary connectivity, without accounting for travel time variation, transfer penalties, or dynamic passenger travel quality. Furthermore, many prior studies focus primarily on considering system reliability from a static perspective,[34,35] overlooking the temporal heterogeneity of traffic patterns, where network reliability can vary significantly across different temporal scales. Temporal fluctuations in demand, travel time, and congestion can significantly affect network performance and user experience, making it essential to assess disruptions with consideration of time variability.

After assessing the reliability of a network, it is essential to propose both effective and feasible measures to enhance its performance, particularly for real-world applications. Much of the existing research aimed at improving network reliability has primarily focused on strategies such as protecting critical nodes or links[36] or adding new nodes and links to the system.[37] However, the practical implementation of these strategies has not been tested with real-world data, and the actual effectiveness of such measures remains uncertain. Moreover, many studies fail to consider the practical factors related to real-world operational scenarios, such as varying traffic patterns and operational dynamics. This gap highlights the need for more comprehensive evaluations that consider not only the theoretical effectiveness but also the practical viability of the proposed solutions in real-world transportation systems.

Considering the challenges discussed above, we propose a novel traffic flow-oriented reliability analysis approach to mitigate the practical limitations of the existing studies. Our approach begins by constructing weighted networks that incorporate commuting time costs and transfer-related factors. Based on this, link centrality and network reliability metrics are developed with consideration of transfer quality. Strategies for enhancing network reliability are then proposed. We select the Shanghai metro system as a representative case study due to its large scale and operational complexity. Leveraging real-world passenger flow data, we perform extensive simulations across various temporal windows and traffic patterns, revealing the significance of travel quality and the repeatability of protected links. Compared with the previous traffic-aware models, our approach offers the following advantages. First, it incorporates time-varying passenger flow data directly into the construction of link centrality and reliability metrics, enabling a more data-driven and granular representation of passenger demand and temporal flow patterns within the network. Second, by accounting for commuting time, transfer penalties, travel quality, and temporal variability, it supports a more realistic and dynamic assessment of network performance under disruptions. Third, it integrates two reliability enhancement strategies to improve its practical value for real-world network planning and protection decision-making.

The remainder of this paper is organized as follows. Section II provides a detailed introduction to the reliability analysis approach for urban transportation networks. In Sec. III, we present the experimental results of the reliability assessment and enhancement strategies applied to the Shanghai metro network. Section IV offers a discussion on the implications of our findings and explores the potential applications of our approach.

II. METHODS

In this section, we present the traffic flow-oriented reliability analysis approach for urban transportation networks. We detail the methods for weighted network construction, traffic flow-oriented link centrality and reliability metrics, and two protection strategies for reliability enhancement. The framework of our approach is illustrated in Fig. 1.

A. Commuting time-informed weighted network model

To accurately assess the performance and reliability of transportation networks, we construct a commuting time-informed weighted network based on the L-space representation.[34] The system is modeled as a weighted graph $G(N, L)$, where each node

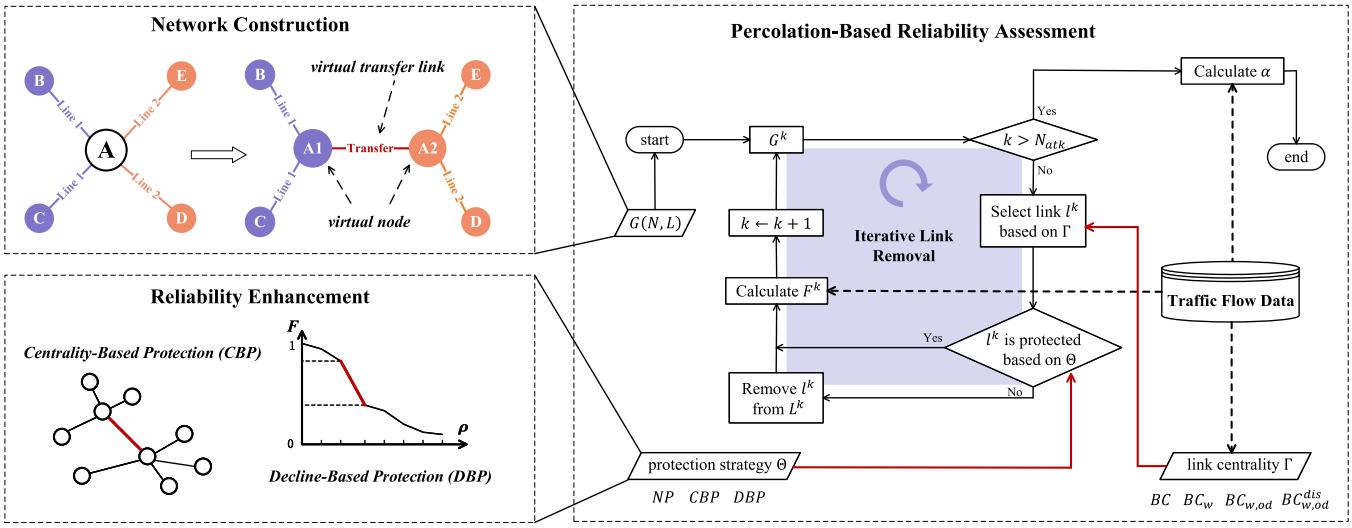

FIG. 1. Framework for traffic flow-oriented transportation network reliability analysis. The top-left section illustrates the diagram of constructing virtual nodes and links for transfer stations during weighted transportation network construction. Here, station A, originally serving as a transfer station between Lines 1 and 2, is divided into two virtual transfer nodes: A1 and A2. A1 and A2 correspond to Line 1 and Line 2, respectively, and the connection between A1 and A2 represents the transfer link between Lines 1 and 2. The right section illustrates the algorithm flow of the percolation-based reliability assessment process. The constructed transportation network, $G(N, L)$, with sets of nodes N and links L, serves as the input. The link removal process iteratively removes unprotected links based on the selected link centrality Γ and protection strategy Θ. When the number of attacked links k reaches the specified threshold N_{atk}, the percolation process ends and the reliability metric α is calculated. The bottom-left section illustrates the two protection strategies for reliability enhancement: centrality-based protection (CBP) strategy and decline-based protection (DBP) strategy, which are incorporated into the reliability assessment algorithm flow.

$n_i \in N$ represents a physical station, and each link $l_{ij} \in L$ denotes a physical connection between stations i and j. This representation preserves the underlying infrastructure topology while aligning with how passengers physically traverse the network. Traditional approaches often simplify the network using topological distances or hop counts, which fail to reflect temporal factors critical to user experience. To address this issue, here we assign weights w_{ij} to each link based on the estimated commuting time. Specifically, for rail-based travel edges, the commuting time represents the scheduled in-vehicle travel time between two connected stations, which can be estimated from the available train schedules or inferred from real-world trip data. Empirical studies have shown that passengers generally follow routes that minimize the total commuting time,[38] and we adopt this behavioral assumption in our model. The shortest commuting time between any origin–destination (O–D) pair is then calculated as the weighted shortest path,

$$\tau_{ij} = \min_{\mathcal{P}_{ij}} \sum_{l_{kl} \in \mathcal{P}_{ij}} w_{kl}, \tag{1}$$

where $\mathcal{P}_{ij}$ represents the set of all feasible paths connecting nodes i and j, and w_{kl} is the commuting time associated with each link along the path.

In rail-based transportation networks, transfer stations often introduce additional delays due to walking, vertical circulation, and crowding. To model these effects, we introduce virtual nodes to represent internal transfer points, connected by virtual transfer links as shown in the top-left section of Fig. 1. This structure enables a more realistic modeling of transfers, which is critical for reliability analysis under disruptions. The weight of each virtual transfer link represents the estimated internal walking time between virtual nodes, determined by the geographic distance and passenger walking speed. A detailed description of the weight calculation method is provided in Appendix A.

B. Traffic flow-oriented link centrality measures

Different transportation network links have varying levels of connectivity and functionality. The disruption of critical hub connections can significantly affect network performance. Traditional betweenness centrality, denoted as BC, is calculated based on the shortest path in terms of the number of hops.[39] However, the length of track segments in transportation networks directly impacts the travel time. Therefore, we replace the shortest hop strategy with the weighted shortest travel path and calculate the weighted betweenness centrality, BC_w, for the links.[40] These centrality measures typically consider the shortest paths between every pair of nodes, without accounting for the frequency differences of various O–D pairs. Some researchers have considered the frequency differences of O–D pairs and calculated node importance based on the shortest hop paths.[32] We extend this idea by incorporating the commuting time costs and formulate the frequencies with traffic flow data. Specifically, we define a traffic flow dataset $\mathcal{D}$ as a collection of O–D pairs, and it is mathematically expressed as

$$\mathcal{D} = \left\{ (s, t, \mu_{s,t}) \mid s, t \in N, \mu_{s,t} \geq 0 \right\}, \tag{2}$$

where s and t are the origin and destination nodes, respectively, and $\mu_{s,t}$ is the flow between stations s and t. We then define the link flow-weighted betweenness centrality, $BC_{w,\mathrm{od}}$, based on the weighted shortest travel path. The quantity $BC_{w,\mathrm{od}}(l_{ij})$ for link l_{ij} is defined as

$$BC_{w,\mathrm{od}}(l_{ij}) = \frac{1}{\mu_{\mathrm{total}}} \sum_{(s,t)\in\mathcal{D}} \frac{\sigma_{s,t|l_{ij}} \mu_{s,t}}{\sigma_{s,t}}, \tag{3}$$

where $\sigma_{s,t}$ represents the number of shortest travel paths between nodes s and t, $\sigma_{s,t|l_{ij}}$ is the number of shortest travel paths between nodes s_t and t_t that pass through link l_{ij}, and $\mu_{s,t}$ and μ_{total} represent the flow between nodes s and t, and the total flow in the network, respectively. The total flow in the network μ_{total} can be expressed as

$$\mu_{\mathrm{total}} = \sum_{(s,t)\in\mathcal{D}} \mu_{s,t}. \tag{4}$$

We also focus on the commuting time-based shortest path length differences between O–D pairs, as short- and long-range O–D pairs have different impacts on network functionality.[31] The three centrality metrics discussed above do not consider these differences. Therefore, we propose a new link centrality metric, $BC^{\mathrm{dis}}_{w,\mathrm{od}}$, which incorporates the shortest commuting time of the O–D pairs. The quantity $BC^{\mathrm{dis}}_{w,\mathrm{od}}(l_{ij})$ for link l_{ij} is defined as

$$BC^{\mathrm{dis}}_{w,\mathrm{od}}(l_{ij}) = \frac{1}{\mu_{\mathrm{total}}} \sum_{(s,t)\in\mathcal{D}} \frac{\sigma_{s,t|l_{ij}} \frac{w_{ij}}{\tau_{s,t}} \mu_{s,t}}{\sigma_{s,t}}, \tag{5}$$

where l_{ij} is the weight of link l_{ij}, and $\tau_{s,t}$ is the shortest travel length between nodes s and t following Eq. (1).

C. Percolation-based reliability assessment

We simulate the link percolation process to assess the reliability of the transportation network. Specifically, percolation here refers to the gradual removal of links from the network and the evaluation of how such disruptions affect the system's overall functionality. We focus on the targeted link removal scenarios, where the links are removed based on a certain centrality measure. As the links are attacked and removed in the percolation process, the network's response is tracked by analyzing the changes in the network performance function. In a previous research, this function was defined as the proportion of unaffected O–D demand. Specifically, if the O–D pairs remain connected despite network attacks, they are considered unaffected.[31] However, this method only considers the existence of a connected path between the O–D pairs and does not account for longer travel times or additional transfers, which may present limitations. Therefore, in this study, we consider the quality attribute of the O–D pairs as $\eta_{s,t} \in [0,1]$, where (s,t) represents a specific O–D pair in $\mathcal{D}$. When the O–D pair is disconnected, $\eta_{s,t} = 0$; otherwise, $\eta_{s,t}$ is defined as the ratio of the travel time $\tau_{s,t}$ before the attack to the travel time $\tilde{\tau}_{s,t}$ after the attack, raised to the power of a constant parameter. Smaller $\eta_{\mathrm{s,t}}$, thus, represents a longer travel time delay, which leads to lower travel quality. As such, we represent the travel quality for the O–D pair (s,t) as

$$\eta_{\mathrm{s,t}} = \left(\tilde{\tau}_{s,t}/\tau_{s,t}\right)^{\beta}, \tag{6}$$

where β is a constant representing the degree of consideration for the travel time variation. As the value of β increases, the variations in travel quality have a more significant influence on the reliability assessment. In contrast, smaller values of β place greater emphasis on the connectivity of travel routes rather than on travel time. When $\beta = 0$, only the O–D's connectivity is considered. We set $\beta = 5$ as a balanced choice that captures moderate sensitivity to service quality changes while avoiding overemphasis on minor delays. A sensitivity analysis is provided in Appendix B to further illustrate the impact of varying β on the reliability assessment results.

The network performance function F is defined as the ratio of the sum of the current quality attributes for all O–D pairs to the total number of O–D pairs, that is,

$$F = \frac{1}{\mu_{\mathrm{total}}} \sum_{(s,t)\in\mathcal{D}} \mu_{s,t}\eta_{\mathrm{s,t}}. \tag{7}$$

Aggregating the quality attributes, the network performance function F effectively represents the overall impact of each step of attack on passenger traveling demand. When $\beta = 0$, F could represent the ratio of unaffected passengers in the entire network after the attack. The changes in F can be recorded through the percolation process. The reliability metric α, connected with the area under the declining F curve,[31] is defined by

$$\alpha = \frac{1}{|V|} \int_0^{|V|} F_\rho \, d\rho, \tag{8}$$

where F_ρ represents the network performance when ρ links have been attacked, and $|V|$ denotes the total number of links removed from the network.

The percolation-based reliability assessment process is illustrated in the right section of Fig. 1.

D. Reliability enhancement strategies

Improving the reliability of transportation networks by strategically protecting or reinforcing specific links is a widely recognized approach in infrastructure planning.[41] In practice, this may involve targeted inspections, deploying on-site maintenance resources, or physical reinforcements to ensure the continuous operability of critical components. To evaluate the effectiveness of protection policies in urban transportation systems, we consider two representative strategies, each based on distinct principles and operational assumptions.

The first approach is the centrality-based protection (CBP) strategy. It prioritizes the protection of links with high topological or functional centrality, under the assumption that these links play dominant roles in maintaining network-wide connectivity and flow. Centrality metrics such as betweenness or flow-weighted importance can be used to rank links for targeted intervention. This approach has been broadly applied in unweighted or purely topological networks,[36] due to its computational efficiency and interpretability. However, its reliability in systems characterized by heterogeneous link weights—such as variable commuting times or passenger flows—requires further investigation.

The second approach is the decline-based protection (DBP) strategy, which iteratively identifies links that contribute most significantly to the deterioration of network performance during the

percolation process.[31,42] This simulation-driven method captures the dynamic impact of link failures by greedily selecting links whose protection most effectively delays the functional collapse of the system. By directly referencing performance loss, DBP offers greater accuracy in prioritizing interventions for complex weighted networks.

CBP offers fast implementation based on precomputed centrality values but may misrepresent actual vulnerability under operational constraints. In contrast, DBP provides a more tailored protection plan, albeit at a higher computational cost due to the need for repeated simulations of the failure-recovery process. In our assessment, we implement and compare both strategies on the same network model to analyze their relative advantages across multiple scenarios.

III. SIMULATION RESULTS

We select the Shanghai metro network as a representative case study for urban transportation network reliability analysis. As one of the world's largest and most complex urban rail transit systems, the Shanghai metro network serves a massive daily ridership exceeding 10 million passengers, generating rich passenger flow dynamics that enable meaningful analysis of traffic-oriented reliability metrics. Through extensive numerical simulations, we evaluate the network's reliability under various attack scenarios, analyze the network performance across different temporal scales, and compare the effectiveness of reliability enhancement strategies.

To demonstrate the scalability of our approach, we also conduct numerical simulations on the metro networks in New York City, Hangzhou, and Shenzhen, with the experimental results presented in Appendix C.

A. Data preparation

The topology of the studied network system is shown in Fig. 2(a). We gather detailed information about the Shanghai metro system, including network and station specifics, as well as the time intervals between trains, from the official Shanghai metro website www.shmetro.com. Using these data, we estimate commuting times based on train arrival intervals to construct the weighted network model. Additionally, we employ a real-world O–D dataset spanning from April 5 to April 12, 2015, which includes smart card transaction records from the Shanghai metro system. This O–D passenger flow dataset forms the foundation for calculating link centrality and reliability metrics in the subsequent simulations. It captures traffic flow data across various traffic patterns, including weekdays (April 7, 8, 9, and 10), weekends (April 6, 11, and 12), and holidays (April 5, Qingming Festival), providing a comprehensive view of the system's performance.

Figure 2(b) presents a comparison of travel time distributions between a weekday (April 9) and a weekend (April 12) utilizing our O–D dataset. The results reveal a significant temporal heterogeneity in travel patterns, with weekend travel featuring more medium and long-distance trips, while weekday travel is characterized by a higher proportion of shorter trips. This difference can be attributed to the variations in trip purpose across the week, which significantly influence travel behavior and temporal patterns.[43] On weekdays, travel is primarily driven by routine commuting between residential areas and workplaces, typically involving shorter trips with fixed schedules. In contrast, weekend travel is often associated with leisure or discretionary activities, which tend to involve longer distances and more varied destinations. This observed temporal heterogeneity underscores the importance of conducting reliability assessments across different temporal scales and traffic patterns.

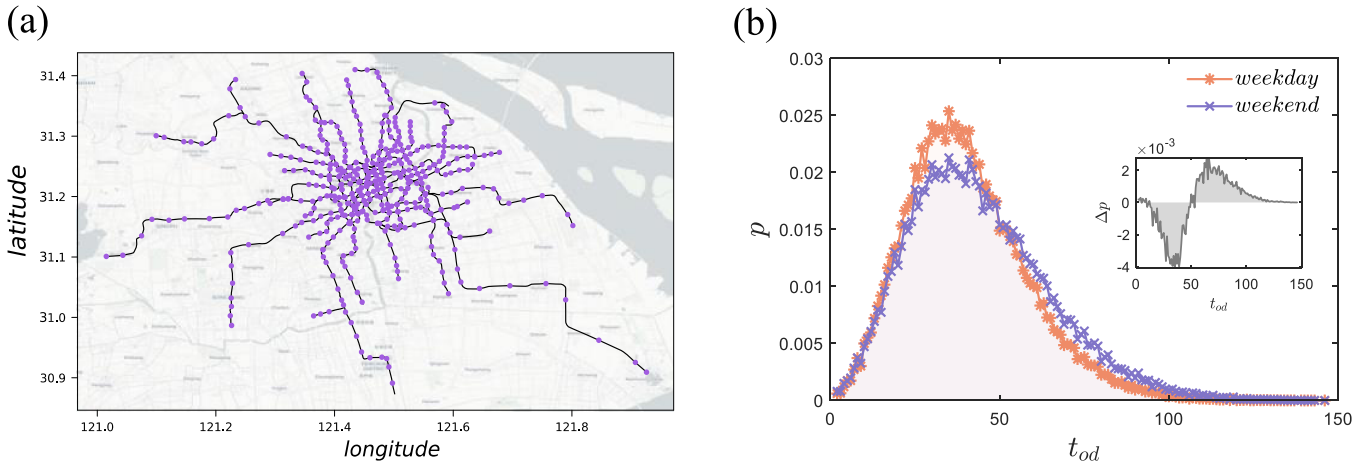

FIG. 2. Illustration of the Shanghai metro system and O–D travel time distribution. (a) The topology of the Shanghai metro network. The purple dots represent the stations and the links represent the tracks. The relative positions of the stations and tracks are arranged according to the actual geographical coordinates. (b) Comparison of the O–D travel time distributions under a weekday (April 9) and a weekend (April 12). The horizontal axis t_{od} represents the travel time in minutes, while the vertical axis p represents the proportion of the O–D pairs. The inset shows the difference in O–D travel time distributions between the weekday and the weekend, calculated as $\Delta p = p_{\text{weekend}} - p_{\text{weekday}}$.

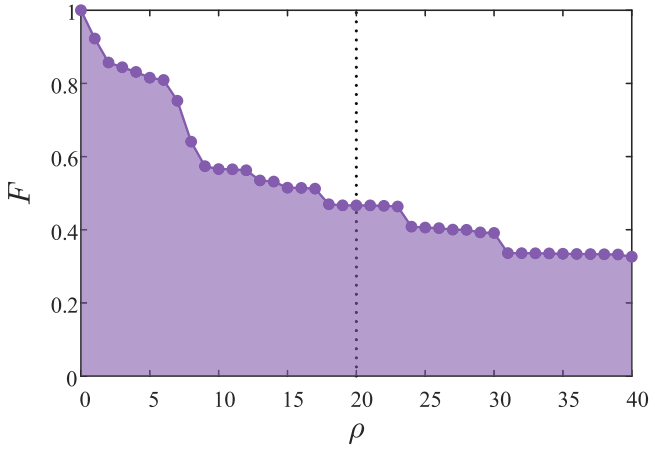

FIG. 3. Line chart depicting the degradation of the network performance function F for the Shanghai metro system during the percolation process (the O–D flow from 7:00 to 8:00 on April 9, $\beta = 5$). The attack is based on the $BC^{\text{dis}}_{w,\text{od}}$ metric, with a removal of 40 links from the Shanghai metro system. Here, the horizontal axis ρ represents the number of attacked links, while the vertical axis represents the network performance function F.

B. Reliability assessment

We conduct a reliability assessment of the Shanghai metro network under different disruption scenarios. We design five link attack strategies, including random attack and deliberate attacks based on different centrality metrics: BC, BC_w, $BC_{w,\text{od}}$, and $BC^{\text{dis}}_{w,\text{od}}$.

We first investigate the decline in the network functionality with a large attack scale. Figure 3 illustrates the decline in the network functionality under deliberate attacks based on the $BC^{\text{dis}}_{w,\text{od}}$ metric, with a removal of 40 links from the network. It can be seen that approximately 65% of the O–D pairs are affected, which rarely happens in real life. It can also be observed that when 20 links are attacked, the proportion of the affected O–D pairs exceeds 50%, and the decline in network performance F becomes significantly slower in the subsequent process. We, therefore, focus on the early phase of the percolation process in the following experiments.

We next conduct extensive experiments involving the stepwise removal of 20 links (approximately 4% of the overall network links). We illustrate F's variations under different attack scenarios and different degrees of consideration for travel quality β in Fig. 4. It can be observed that when $\beta = 0$, considering only connectivity, F remains at 1, even if the three links with the highest $BC_{w,\text{od}}$ values are disconnected. This contradicts the practical experience, as the disconnection of the critical links typically significantly impacts a system's functionality. As β increases from 1 to 9, indicating a higher emphasis on travel time variation, the rate of decline in the network function F accelerates. This finding suggests that considering only the O–D connectivity may underestimate the network's vulnerability. Specifically, when $\beta = 0$, the deliberate attack of 20 links based on $BC^{\text{dis}}_{w,\text{od}}$ disrupts about 49% of the O–D connections, affecting approximately 3.16×10^6 travel demands. With $\beta = 5$, it results in a 53% decline in the network function, and with $\beta = 9$, the decline is 55%. This indicates that the transportation network suffers severe impacts when a small part of the links are attacked. While the disconnection of the O–D remains the primary factor in the decline of the network function, the impact on the trip quality is also significant and should not be underestimated. Thus, we set β as 5 in the subsequent reliability assessment.

Figure 5 displays the time-varying reliability metrics within one day under different attack strategies and traffic patterns (weekday, weekend, and holiday). For each traffic pattern, it can be observed that the deliberate attacks significantly reduce the reliability metric compared to the random attack. This suggests a high degree of heterogeneity in link importance within the weighted network derived from traffic flow data, underscoring the significance for designing centrality metrics to locate vulnerable links. Among the deliberate attack strategies, it can be seen that the network reliability significantly decreases under the attack based on the $BC^{\text{dis}}_{w,\text{od}}$ compared to BC, BC_w, and $BC_{w,\text{od}}$. Through calculating the daily average reliability metrics, the network reliability decreases by 21.7% under BC attacks, 21.6% under BC_w attacks, 23.8% under $BC_{w,\text{od}}$ attacks, and 30.8% under $BC^{\text{dis}}_{w,\text{od}}$ attacks in the weekday case (April 9). These findings illustrate the advantages of $BC^{\text{dis}}_{w,\text{od}}$ in identifying the critical links that significantly affect the network reliability. We next compare the time-varying reliability curves under different traffic patterns. We observe that the reliability metric exhibits slight decreases and greater temporal fluctuations during weekends and holidays, likely attributable to the expansion of O–D ranges on non-working days, as passengers tend to undertake longer-distance trips on weekends and holidays. We further computed Pearson correlation coefficients among the reliability variation curves across eight consecutive days (April 5–April 12) incorporating three traffic patterns, and visualized the results as a heat-map in Fig. 5(d). The results demonstrate that Pearson's correlation coefficients are higher within weekdays and non-working days, but relatively lower between the two. This suggests that transportation operators should adopt targeted maintenance and operational strategies based on the type of day.

C. Reliability enhancement

We investigate the reliability improvement of the Shanghai metro system under partial link attacks when protection strategies, CBP and DBP, are taken into account. The proportion of the protected links is set to approximately 1% of the total number of network links.[31] Specifically, the attack scale is set to 20 links, with 5 of those links being strongly protected to ensure they are unaffected by the attacks. According to the CBP strategy, in the attack scenarios based on BC, BC_w, $BC_{w,\text{od}}$, and $BC^{\text{dis}}_{w,\text{od}}$, we protect the top five links with the highest centrality values, which are the same as the attack method. For the DBP strategy, we simulate the decline in the network performance function F under the attack scenarios based on BC, BC_w, $BC_{w,\text{od}}$, and $BC^{\text{dis}}_{w,\text{od}}$. In each attack scenario, we identify and protect the five links that cause the fastest decline in F. Finally, the reliability α is calculated to evaluate the effectiveness of the protection strategies.

We summarize the daily average reliability index values of the Shanghai metro system in Table I and plot the reliability variation curves in Fig. 6. The results reveal distinct performance advantages

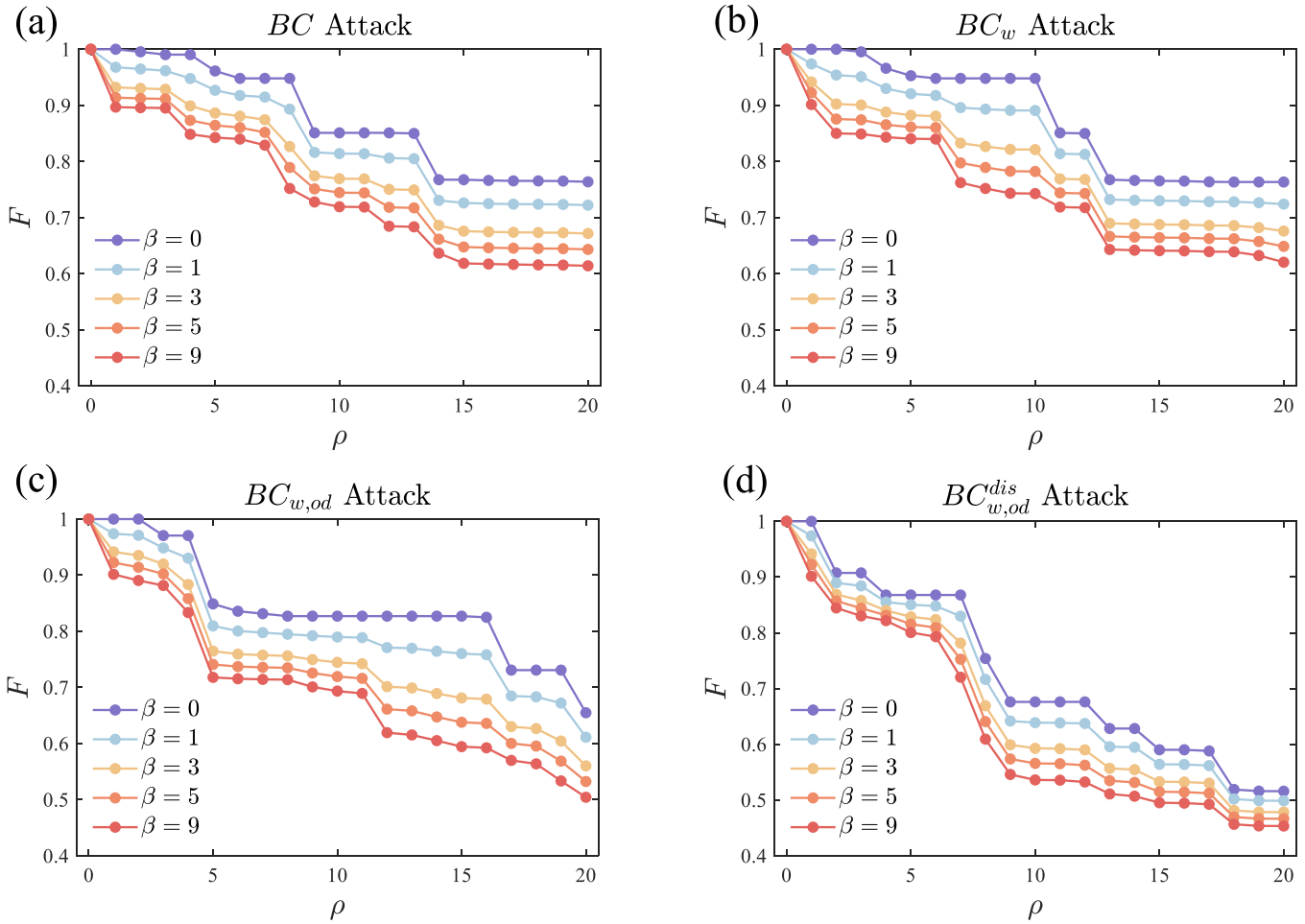

FIG. 4. Percolation-based simulation results of the Shanghai metro system. The line charts depict the degradation of the Shanghai metro network function F during the percolation process with different attack strategies (the O–D flow from 7:00 to 8:00 on April 9). The horizontal axis ρ represents the number of attacked links, while the vertical axis represents the network performance function F specified in Eq. (7). (a) Deliberate attack based on BC. (b) Deliberate attack based on BC_w. (c) Deliberate attack based on $BC_{w,od}$. (d) Deliberate attack based on $BC^{dis}_{w,od}$.

between CBP and DBP when subjected to different attack strategies. For the average daily reliability values, under BC, BC_w, $BC_{w,od}$, and $BC^{dis}_{w,od}$ attack scenarios, the reliability using CBP increases by 6.99%, 5.59%, 7.47%, and 11.12%, respectively, compared to the unprotected scenario (NP). In contrast, under DBP, the reliability increases by 2.00%, 2.23%, 3.49%, and 15.21%, respectively, compared to NP. Therefore, the CBP strategy, which utilizes the same centrality measure as the attack strategy, is rather effective in enhancing the network reliability under the attack scenarios based on BC, BC_w, and $BC_{w,od}$. Though less useful for the $BC^{dis}_{w,od}$ attack situation, we conclude that the CBP strategy exhibits more stable performance across different attack scenarios compared with the DBP strategy.

Additionally, we investigate the protective effects using both protection strategies based on $BC^{dis}_{w,od}$ under different attack scenarios. That is, we protect links based on the $BC^{dis}_{w,od}$ values and the corresponding simulation results, disregarding the actual attack strategy. This approach is more realistic in real-world scenarios, as the attack strategy is often unknown. We note that protective measures adopted in this part might safeguard the links that are not actually under attack, potentially rendering some protective measures ineffective. Using the real traffic data from 7:00 to 8:00 on Day 9 as an example, the CBP protection strategy based on the top five $BC^{dis}_{w,od}$ resulted in four effective protected links under the attack scenarios of BC, BC_w, and $BC_{w,od}$. The link from Longyang Road to Zhangjiang High-tech Park, which ranked 3rd, was not protected

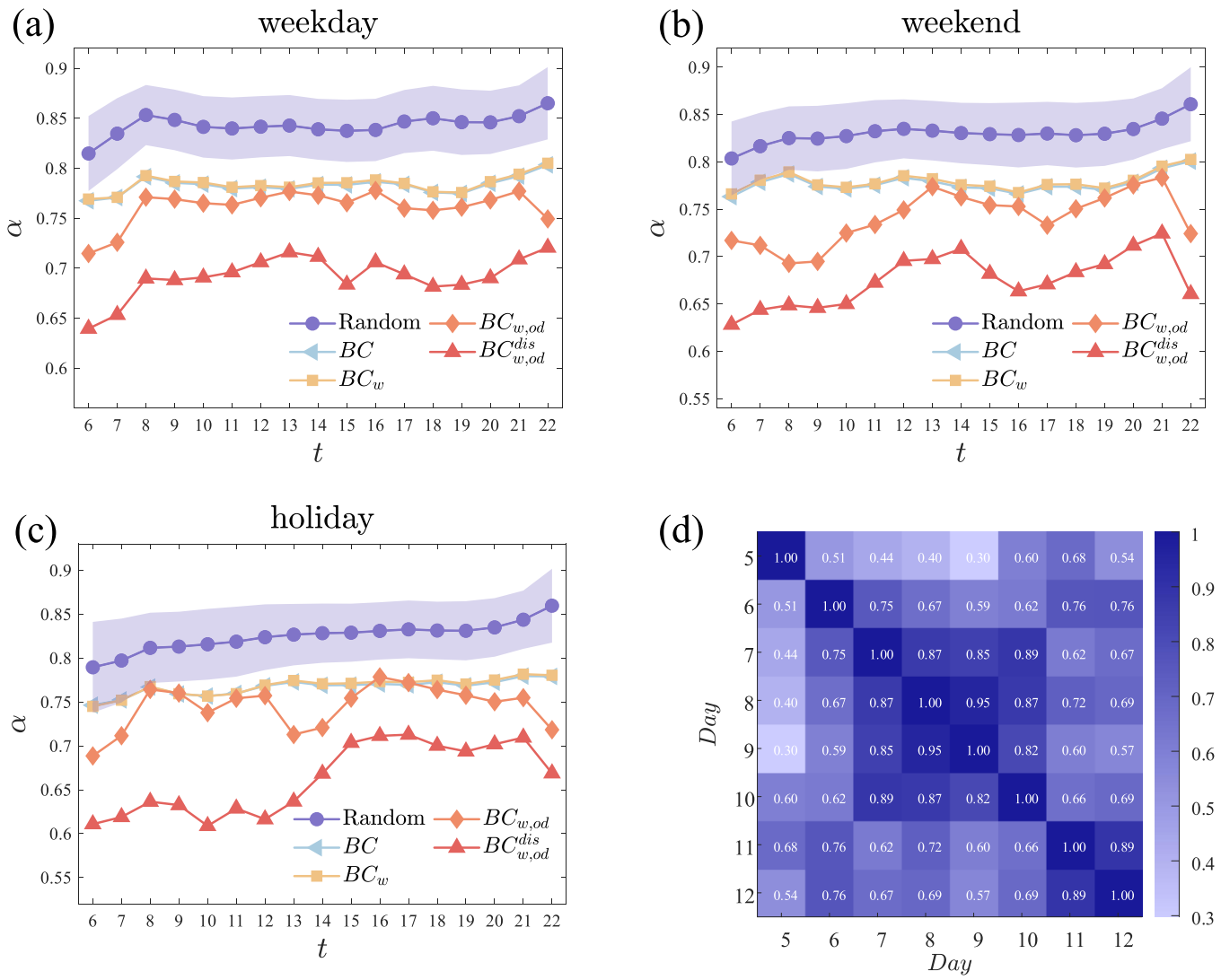

FIG. 5. Reliability assessment results of the time-varying reliability metrics under different attack strategies and traffic patterns (the O–D flow from 6:00 to 23:00). The considered attack strategies include random attack and deliberate attacks based on BC, BC_w, $BC_{w,od}$, and $BC^{dis}_{w,od}$, and the traffic patterns include a weekday, weekend, and holiday. For the results under random attacks, the light purple shaded area represents the standard deviation computed over 30 independent simulation runs. (a) Reliability variation curve on a weekday, April 9. (b) Reliability variation curve on a weekend, April 12. (c) Reliability variation curve on a holiday, April 5. (d) Heat-map of the Pearson's correlation coefficients of the reliability metrics across different days, incorporating the traffic patterns of weekdays (April 7, April 8, April 9, and April 10), weekends (April 6, April 11, and April 12) and a holiday (April 5).

in any of these three attack scenarios. This link ranked 101st, 94th, and 23rd in the BC, BC_w, and $BC_{w,od}$ scenarios, indicating its limited significance in terms of structural betweenness. However, when considering the O–D demand, its importance increases, especially when we take the O–D distance into account, making it even more crucial. Figure 6 shows the resulting reliability curves with markers $CBP - BC^{dis}_{w,od}$ and $DBP - BC^{dis}_{w,od}$. Interestingly, we observe that $CBP - BC^{dis}_{w,od}$ also exhibits better protection efficacy compared with $DBP - BC^{dis}_{w,od}$ under the attack scenarios of BC, BC_w, and $BC_{w,od}$. This further indicates the stability of centrality-based protection strategies under different attack scenarios.

If the protected links show consistency under similar traffic patterns, there is no need for real-time calculation of the protection links based on current traffic, nor is there a requirement to mobilize

TABLE I. Daily average reliability index α values of the Shanghai metro system under different protection strategies and attack scenarios. The column headers represent attack scenarios, while the row headers represent protection strategies. Each attack scenario corresponds to two columns of the data: the left column indicates the reliability index values, and the right column indicates the percentage increase in the reliability index compared to the cases with no protection (NP).

	BC		BC_w		$BC_{w,\mathrm{od}}$		$BC^{\mathrm{dis}}_{w,\mathrm{od}}$	
NP	0.7828	…	0.7842	…	0.7616	…	0.6918	…
CBP	0.8376	6.99%	0.8281	5.59%	0.8184	7.47%	0.7688	11.12%
DBP	0.7985	2.00%	0.8018	2.23%	0.7881	3.49%	0.7970	15.21%
CBP-$BC^{\mathrm{dis}}_{w,\mathrm{od}}$	0.8203	4.79%	0.8231	4.96%	0.8209	7.79%	…	…
DBP-$BC^{\mathrm{dis}}_{w,\mathrm{od}}$	0.7947	1.52%	0.7999	2.00%	0.8080	6.09%	…	…

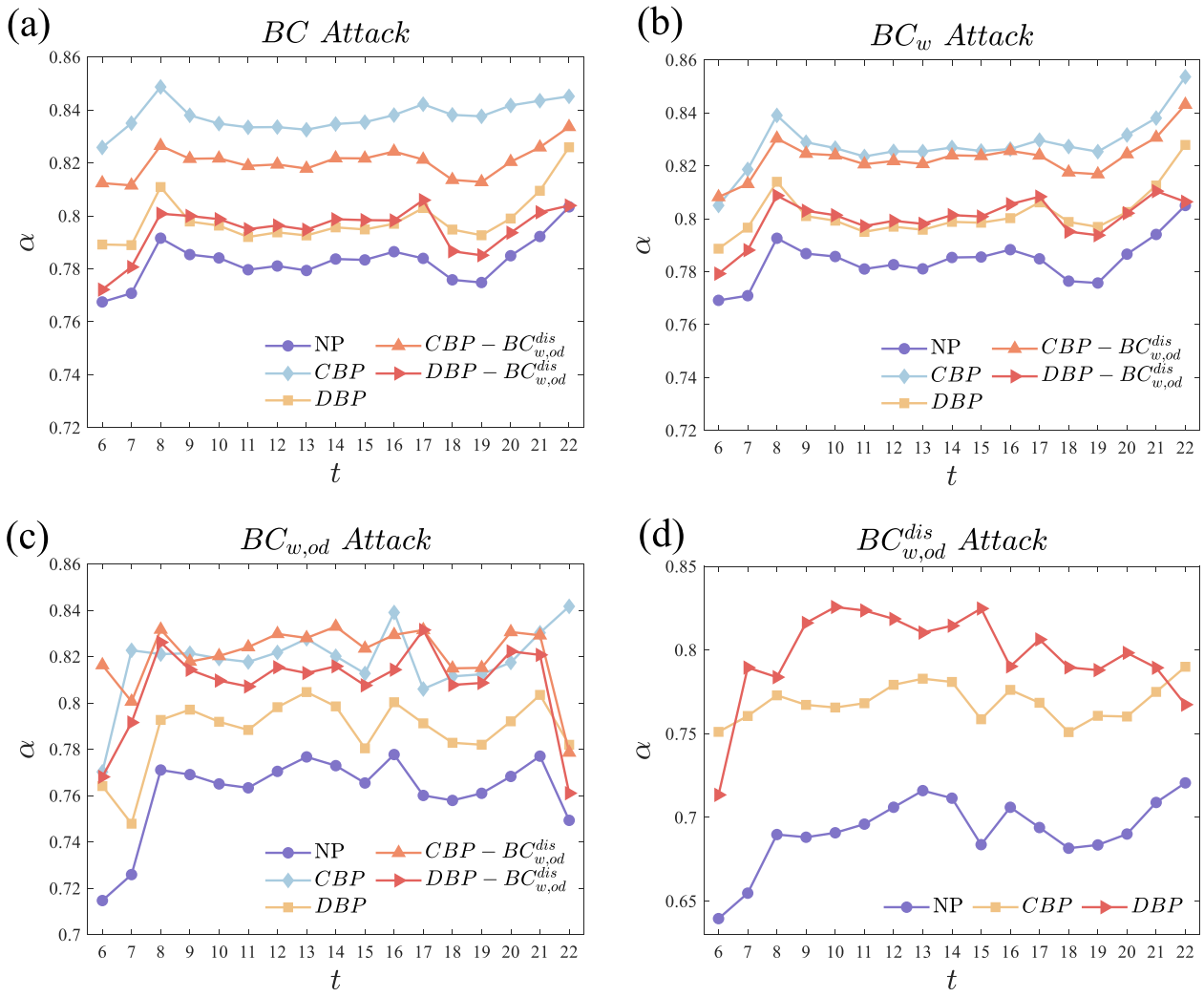

FIG. 6. Time-varying line charts of reliability metrics for the Shanghai metro system under different protection strategies and attack scenarios. In the legend panel, NP indicates no protection measures, CBP represents the centrality-based protection measure (using the same centrality measure as the attack scenario), DBP represents the decline-based protection measure (using the same centrality measure as the attack scenario), CBP-$BC^{\mathrm{dis}}_{w,\mathrm{od}}$ indicates the centrality-based protection measure using $BC^{\mathrm{dis}}_{w,\mathrm{od}}$ centrality, and DBP-$BC^{\mathrm{dis}}_{w,\mathrm{od}}$ indicates the decline-based protection measure using $BC^{\mathrm{dis}}_{w,\mathrm{od}}$ centrality. (a) Under the BC attack scenario. (b) Under the BC_w attack scenario. (c) Under the $BC_{w,\mathrm{od}}$ attack scenario. (d) Under the $BC^{\mathrm{dis}}_{w,\mathrm{od}}$ attack scenario.

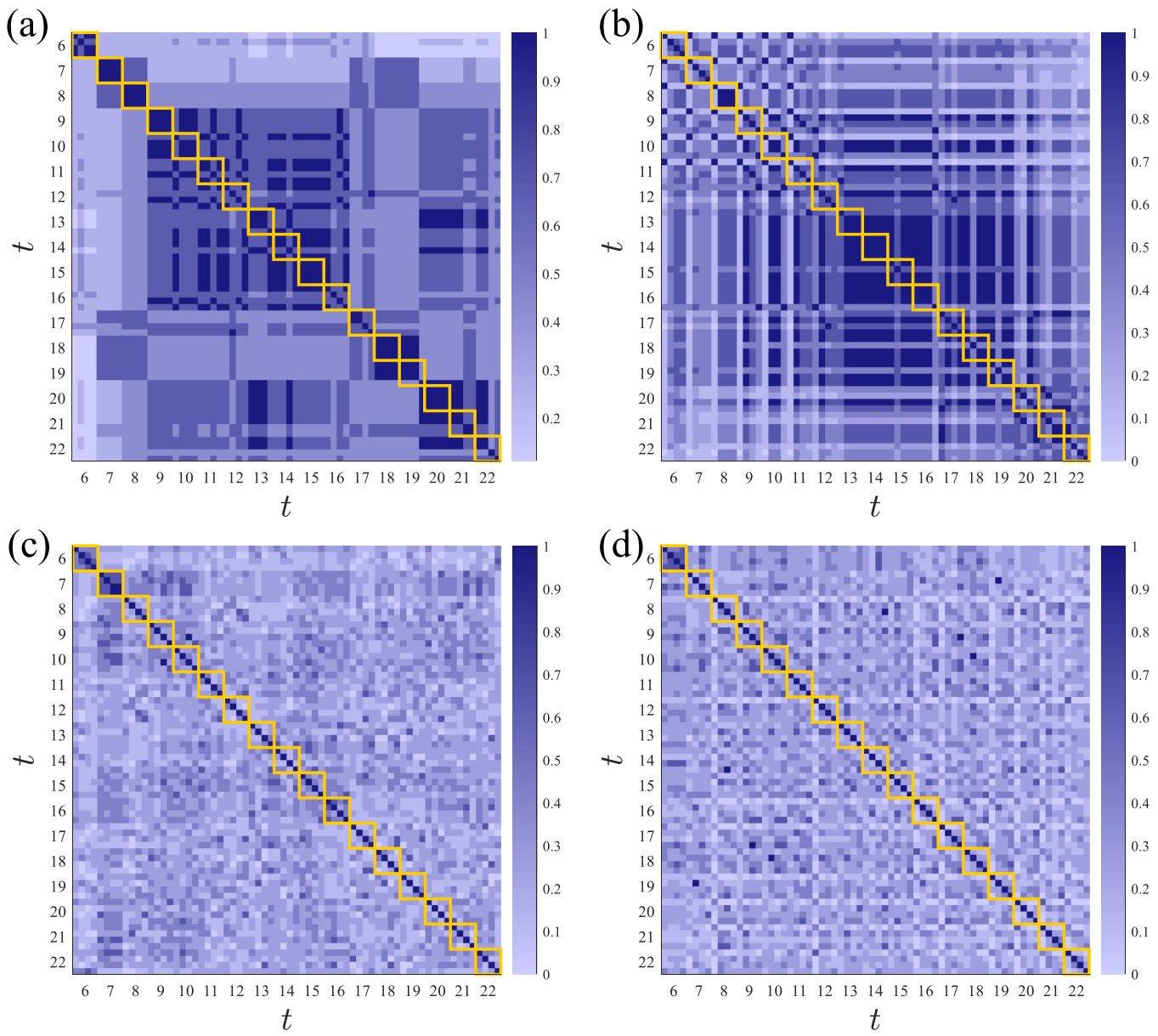

FIG. 7. Heat-map of the overlap rates of the protected links under different protection strategies on weekdays in the Shanghai metro system. The horizontal and vertical axes represent the time range from 6:00 to 23:00, with each hour represented as one cell. Each cell contains a 4×4 heat-map, where the value of each point in the heat-map is given by the overlap rate results of the $BC^{\text{dis}}_{w,\text{od}}$ metric for the corresponding time periods. The cells along the main diagonal are highlighted by yellow boxes, representing the consistency strength of the protected links across different days. (a) Overlap rates based on the CBP strategy during weekdays, using the real O–D data on April 7, April 8, April 9, and April 10. (b) Overlap rates based on the CBP strategy during non-working days, using the real O–D data on April 5, April 6, April 11, and April 12. (c) Overlap rates based on the DBP strategy with the aforementioned weekday O–D data. (d) Overlap rates based on the DBP strategy with the aforementioned O–D data from non-working days.

significant resources in real time to handle failures. This can greatly enhance the practical significance of the study. We calculate the sets of the protected links under the CBP and the DBP protection strategies based on the $BC^{\text{dis}}_{w,\text{od}}$ metric for different traffic patterns. By computing the overlap rate of the protected links, we characterize the degree of consistency of the protection strategies across different traffic patterns. The results of heat-map of the overlap rates for the protected links are illustrated in Fig. 7. We can observe

the consistency strength of the protected links across different days through the depth of color in the cells where the time periods of the horizontal and vertical coordinates are aligned, i.e., the cells along the main diagonal highlighted by yellow boxes. It is evident that the overlap rates of the protected links under the CBP strategy, shown in the upper two plots, are significantly higher than those under the DBP strategy, depicted in the lower two plots. The absence of overlapped protected links under *DBP* indicates that the links that most decline in F during the percolation processes are not consistently the same despite relatively stable traffic patterns. This further suggests that employing the CBP strategy makes it feasible to utilize the historical traffic data to calculate the required protected links, significantly enhancing the practical usefulness of the CBP protection strategy proposed in this article. In contrast, the DBP strategy may face challenges in this regard. Therefore, the CBP strategy, based on the $BC^{\mathrm{dis}}_{w,\mathrm{od}}$ metric, demonstrates both the protection effectiveness and the repeatability of the protected links under similar traffic patterns. Consequently, it is deemed more suitable for enhancing reliability in real-world scenarios.

IV. DISCUSSION

In this study, we introduce an innovative traffic flow-oriented reliability analysis approach tailored for transportation network systems, which integrates both structural and functional aspects of network performance. By constructing weighted networks that incorporate transfer factors and proposing novel link centrality metrics and reliability measures, we effectively assess the impact of topological changes on network reliability through percolation-based numerical simulations. Furthermore, we design and evaluate two reliability enhancement strategies, demonstrating their practical applicability and repeatability under different temporal scales and traffic patterns. These methodological advancements provide a comprehensive and realistic approach to assessing and enhancing transportation system reliability.

Our experimental results demonstrate that the Shanghai metro system exhibits significant vulnerability under deliberate attacks, particularly when critical links are targeted based on the proposed $BC^{\mathrm{dis}}_{w,\mathrm{od}}$ metric. The decline in network performance F is more pronounced when travel quality is considered, emphasizing the importance of incorporating travel time and transfer factors into reliability assessments. Furthermore, the proposed protection strategies effectively mitigate the impact of attacks, with the centrality-based protection (CBP) strategy with $BC^{\mathrm{dis}}_{w,\mathrm{od}}$ showing high repeatability and practical applicability under similar traffic patterns. These findings highlight the necessity of integrating functional metrics and targeted protection strategies into transportation system planning and management to enhance resilience and ensure reliable urban transportation services.

This work demonstrates that passenger flow data improve the assessment of transportation system functionality by capturing actual travel patterns, demand distributions, and temporal variations, revealing critical links and vulnerabilities that may not be apparent in theoretical models. However, real-world origin–destination data remain difficult to obtain due to limitations in data coverage, heterogeneity across sources, and privacy concerns.[44] These challenges hinder large-scale analyses of transportation system performance. To address this, future research should focus on developing comprehensive simulation frameworks that replicate real-world transportation dynamics with high fidelity. In particular, integrating reliability analysis into cyber-physical systems[45] offers a valuable solution. Furthermore, another promising direction for future research lies in integrating the spatiotemporal evolution of transportation networks into our reliability analysis framework. As urban rail systems undergo continuous expansion and operational changes, these dynamics significantly impact service reliability, including delay propagation, vulnerability to disruptions, and overall system resilience.[3,46] Capturing both the topological and temporal aspects of network development would enable a more nuanced understanding of how structural changes influence traffic patterns and reliability metrics over time. By aligning traffic flow analysis with evolving network configurations, future studies can better quantify the reliability of transportation systems under realistic, time-varying conditions, ultimately supporting the design of more reliable and adaptive transit operations.

ACKNOWLEDGMENTS

We gratefully acknowledge Chao Yang, Wangzhe Gui, Huiyu Zhi, Zhiwen Ren, and Xu Zhang for providing some information and methods during the research discussion. We also acknowledge the support of the National Natural Science Foundation of China (NSFC) (Grant Nos. 11875133, 11075057, and 12147101) and the National Key R&D Program of China (Grant No. 2018YFB2101302).

AUTHOR DECLARATIONS

Conflict of Interest

The authors have no conflicts to disclose.

Author Contributions

Yihong Bao and Qihang Chen contributed equally to this work.

Yihong Bao: Data curation (equal); Software (equal); Writing – original draft (equal). **Qihang Chen:** Data curation (equal); Validation (equal); Visualization (equal); Writing – review & editing (equal). **Dingding Han:** Conceptualization (equal); Methodology (equal); Supervision (equal); Visualization (equal); Writing – review & editing (equal).

DATA AVAILABILITY

The data that support the findings of this study are available from the corresponding author upon reasonable request.

APPENDIX A: CALCULATION OF VIRTUAL TRANSFER LINK WEIGHTS

In the weighted network model constructed in Sec. II A, the link weights represent the time cost required for a passenger to traverse each link. For virtual transfer links, the weight corresponds to

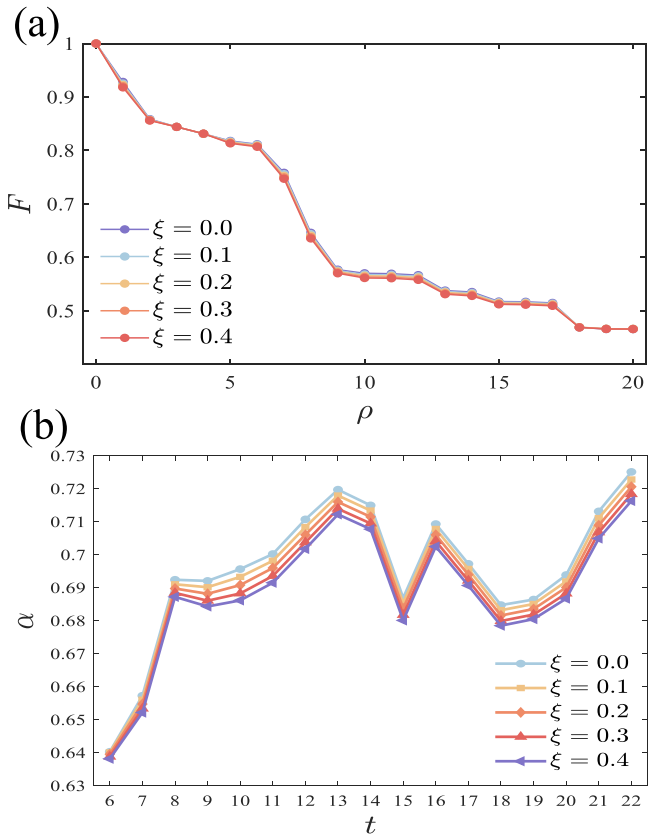

FIG. 8. Impact of different speed reduction rates ξ on the network function F and reliability metric α. The results are simulated under deliberate attack based on $BC^{dis}_{w,od}$ centrality. (a) Network function F under different speed reduction rates ξ using O–D flow data on April 9, 7:00–8:00. (b) Reliability metric α under different speed reduction rates ξ using O–D flow data on April 9.

the walking time needed for a passenger to pass through the transfer corridor. For a specific virtual transfer link l_{ij}, we assume that passengers move at a constant speed v_w. The length of the transfer corridor is denoted by d^{geo}_{ij}, which represents the spherical distance between the corresponding virtual nodes based on their geographic coordinates. Accordingly, the weight is calculated as

$$w^{transfer}_{ij} = \frac{d^{geo}_{ij}}{v_w}. \tag{A1}$$

Estimating passenger walking speed v_w within transfer corridors is a nontrivial task, as it is affected by various factors such as corridor width, congestion level, and ease of movement, which differ across stations. To simplify the calculation, this study adopts a typical walking speed of 1.55 m/s, based on the statistical findings reported in Zhang *et al.*,[47] assuming it reflects a representative walking pace in transfer environments. To test how this simplification might affect our reliability analysis, we also considered the impact of crowding on passenger movement speed. Following the estimated fundamental diagram of pedestrian flow in a straight corridor,[47] we implemented a piecewise speed formula that accounts for density-dependent velocity,

$$v_w(\rho) = \begin{cases} \bar{v_w} & \text{if } \rho \le \bar{\rho}, \\ \max(\bar{v_w} - \xi(\rho - \bar{\rho}), 0.3) & \text{if } \rho > \bar{\rho}, \end{cases} \tag{A2}$$

where $\bar{v_w}$ represents the nominal walking speed, and we set $\bar{v_w} = 1.55$; ρ represents the estimated pedestrian density, which is calculated as the number of origin–destination pairs passing through this link divided by the length of the link; $\bar{\rho}$ represents the critical density threshold above which speed begins to decrease, and we set $\bar{\rho} = 2$; ξ represents the rate of speed reduction per unit increase in density. We tested the impact of different speed reduction rates ξ on the reliability analysis results, and plotted the results in Fig. 8. The results show that variations in ξ do not significantly affect the overall trends of both the network function F and the reliability metric α. This can be attributed to the relatively small proportion of virtual transfer links compared to the physical links in the network. The majority of travel time cost is determined by the weights of the actual physical links; so perturbations to virtual link weights have a limited impact on the overall results. This indicates that our reliability analysis findings are robust against the constant speed assumption for passengers in transfer corridors.

APPENDIX B: SENSITIVITY ANALYSIS OF PARAMETER β

The parameter β in Eq. (6) controls the weight placed on travel time variation in the reliability assessment. Larger values emphasize travel quality degradation, while smaller values focus more on route connectivity. We set $\beta = 5$ as a balanced basis that reflects both aspects. To further examine the influence of this parameter, we conduct a sensitivity analysis over the interval [4,6], which captures a representative range around the baseline setting and allows us to observe the stability of the reliability outcomes under moderate variation.

Figure 9 illustrates the impact of varying the parameter β on the network function F and the reliability metric α, as well as the effectiveness of the CBP and DBP protection strategies under deliberate attacks based on $BC^{dis}_{w,od}$. The results show that the value of β affects the absolute values of both the network function F and the reliability metric α, with larger β leading to lower values of F and α. The results show that the value of β affects the absolute values of both the network function F and the reliability metric α, with larger β leading to lower values of F and α. However, the overall trends of both curves remain highly consistent, and the qualitative conclusions obtained in Sec. III do not change. This supports the appropriateness of setting $\beta = 5$ as a balanced and representative value in the main analysis and indicates that the reliability assessment results in this study are robust to the variations in the parameter β.

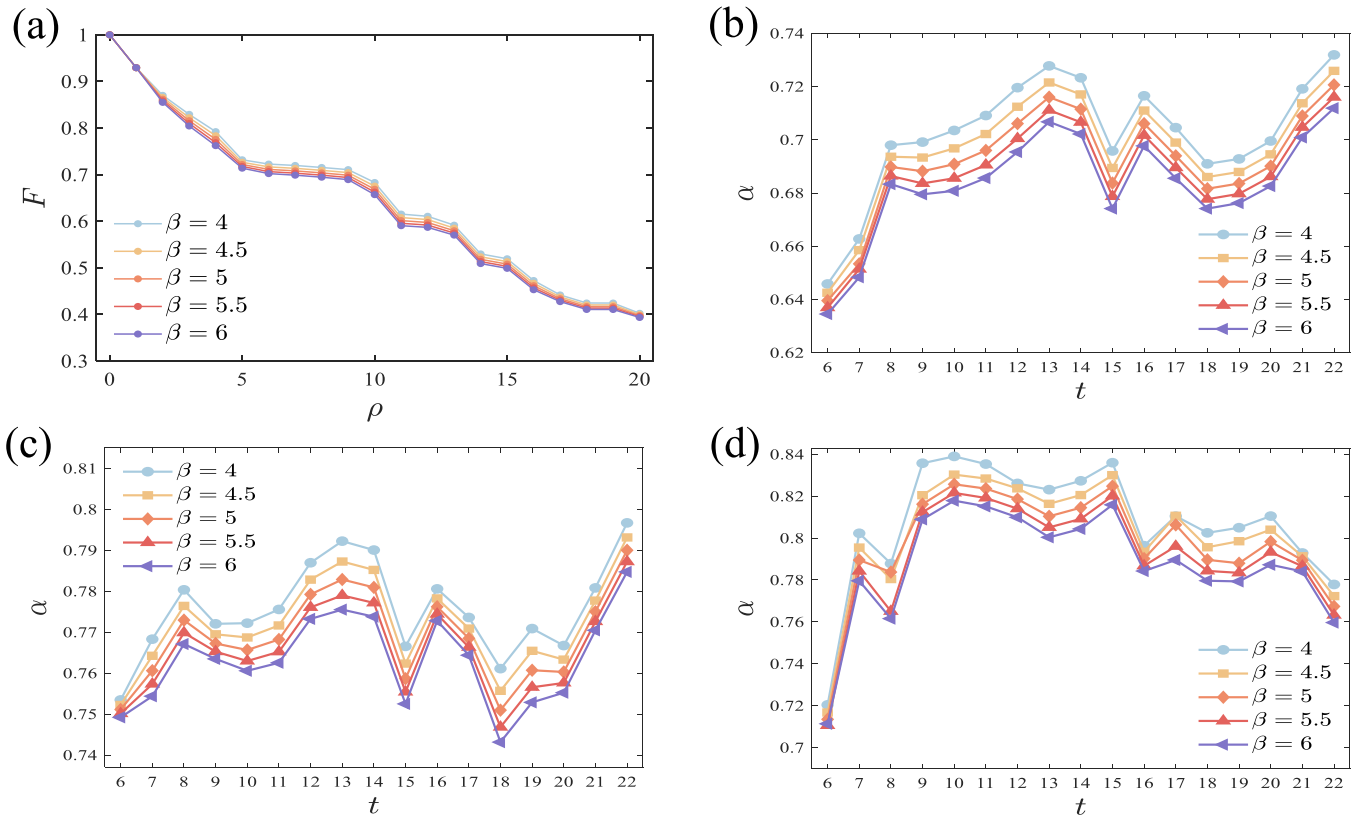

FIG. 9. Sensitivity analysis of parameter β. The results are simulated under deliberate attack based on $BC^{dis}_{w,od}$ centrality. (a) Network function F under different β using O–D flow data on April 9, 7:00–8:00. (b) Reliability metric α with no protection under different β using O–D flow data on April 9. (c) Reliability metric α with the *CBP* protection strategy under different β using O–D flow data on April 9. (d) Reliability metric α with the *DBP* protection strategy under different β using O–D flow data on April 9.

APPENDIX C: EXTENDED EXPERIMENTAL RESULTS ACROSS MULTIPLE CITIES

To demonstrate the scalability of the proposed reliability assessment and enhancement method, we provide additional experimental results based on real-world data from three urban metro network systems. Specifically, we analyze the reliability of the New York City metro in 2024, the Hangzhou metro in 2019, and the Shenzhen metro in 2018. Figures 10(a)–10(c) illustrate the actual geographical topologies of the three studied metro networks.

We plotted the variation curves of the network functionality F under the $BC^{dis}_{w,od}$-based targeted attack strategy in Figs. 10(d)–10(f), where 20 links were sequentially removed. As can be observed, the overall trend of the curves demonstrates a gradually decreasing rate of decline, which is consistent with the results for the Shanghai metro shown in Fig. 3 of the main text. These results indicate that the deliberate attack strategy based on the proposed $BC^{dis}_{w,od}$ centrality effectively prioritizes the removal of globally vulnerable links under realistic passenger flow scenarios, leading to a rapid initial degradation of network functionality. Moreover, among the three cities, the reliability of the Hangzhou metro network experiences a notably sharp decline in the early stage, followed by a more gradual reduction, in contrast to the New York and Shenzhen metro networks. This observation can be attributed to the relatively small size, lower structural complexity, and fewer functionally critical links in the Hangzhou metro network, making it more susceptible to rapid breakdown under $BC^{dis}_{w,od}$-based targeted attacks.

To further assess the reliability of metro networks, we plotted the variation curves of reliability metrics for the three cities under random attacks as well as four targeted attack strategies, as shown in Figs. 11(a)–11(c). The results indicate that, in all three cities, the reliability curves under the $BC^{dis}_{w,od}$-based targeted attack consistently appear at the lowest position, reflecting the most severe degradation in network reliability. This observation aligns with the findings for the Shanghai metro presented in Fig. 5, further confirming the effectiveness of the $BC^{dis}_{w,od}$-based strategy. It is worth noting that, unlike the Shanghai and New York metro networks, the Shenzhen and Hangzhou networks exhibit higher reliability under certain random attack simulations compared to the targeted attacks based on BC and BC_w centrality. In other words, random attacks could lead to more severe network degradation than BC-based and BC_w-based targeted attacks in certain cases. This observation suggests that traditional topology-based centrality measures, such as BC and BC_w, may fail to accurately identify the truly critical links in transportation systems.

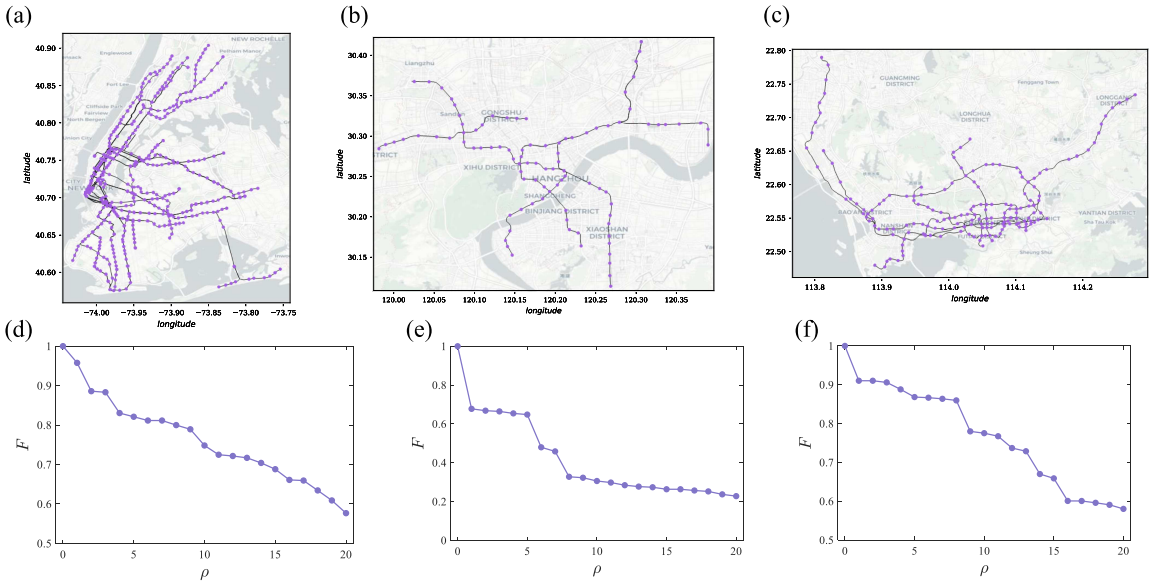

FIG. 10. Illustration of three urban metro network topologies and percolation-based simulation results. (a)–(c) illustrate the topology of the New York City metro network in 2024, the Hangzhou metro network in 2019, and the Shenzhen metro network in 2018, respectively. The purple dots represent the stations and the links represent the tracks. (d)–(f) depict the degradation of the network performance function F under $BC^{dis}_{w,od}$-based targeted attack, with New York City metro O–D flow data from 7:00 to 8:00 on April 12, 2024, Hangzhou metro O–D flow data from 7:00 to 8:00 on January 4, 2019, Shenzhen metro O–D flow data from 7:00 to 8:00 on September 1, 2018, respectively.

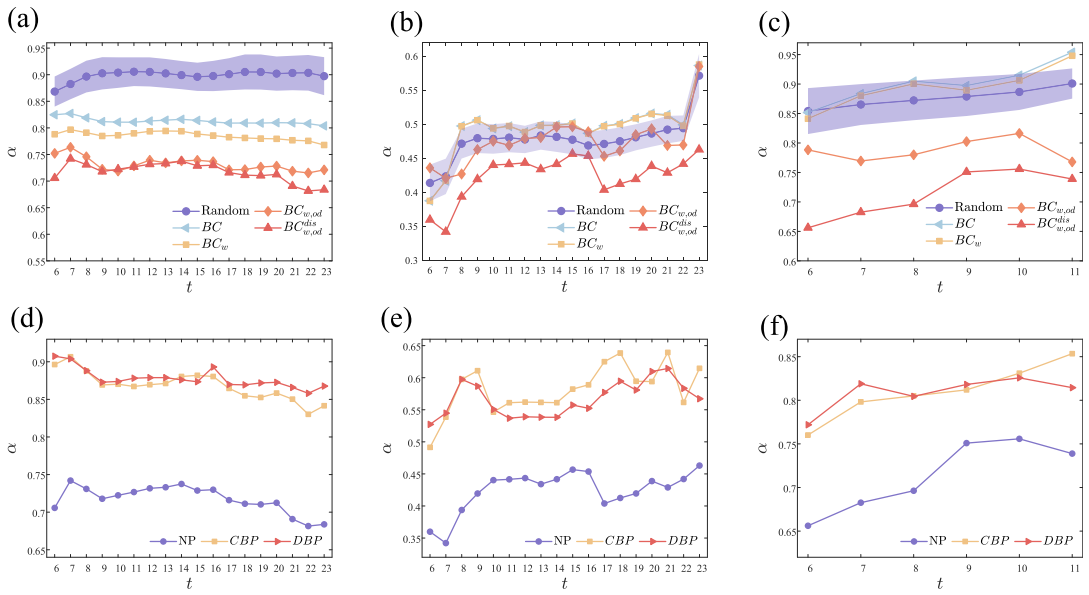

FIG. 11. Time-varying line charts of reliability metrics for three metro systems under different attack and protection strategies. The considered attack strategies include random attacks and deliberate attacks based on BC, BC_w, $BC_{w,od}$, and $BC^{dis}_{w,od}$. For the results under random attacks, the light purple shaded area represents the standard deviation computed over 30 independent simulation runs. The considered protection strategies include no protection strategy (NP), centrality-based protection (CBP) and decline-based protection (DBP). (a)–(c) depict the reliability variation curves under different attack strategies with O–D data from the New York City Metro system on April 12, 2024, Hangzhou metro system on January 4, 2019, and Shenzhen metro system on September 1, 2018, respectively. (d)–(f) illustrate the reliability variation curves under the $BC^{dist}_{w,od}$-based attack with different protection strategies, using O–D data from the New York City, Hangzhou, and Shenzhen metro systems, respectively, corresponding to the same dates as in (a)–(c).

It highlights the potential limitations of purely topological reliability analysis methods and underscores the necessity of incorporating passenger flow data for a more realistic assessment.

To enhance network reliability, we conducted experiments applying both centrality-based protection (CBP) and decline-based protection (DBP) strategies under targeted attacks based on $BC^{dis}_{w,od}$ centrality for the metro networks of the three cities. The corresponding results are shown in Figs. 11(d)–11(f). The results demonstrate that, compared to the unprotected baseline, both protection strategies significantly improve the reliability curves, indicating enhanced robustness. Furthermore, across all three cities, the CBP and DBP strategies exhibit comparable performance overall, and both approaches consistently yield favorable outcomes.

The experimental results from the three cities demonstrate that the proposed reliability assessment and enhancement approach exhibit good scalability across diverse urban transportation systems. The proposed link centrality measures effectively identify the critical links in different network structures, while the protection strategies consistently improve system reliability under various attack scenarios.

REFERENCES

[1]B. P. Loo and K. Y. Leung, "Transport resilience: The occupy central movement in Hong Kong from another perspective," Transp. Res. A: Policy Pract. **106**, 100–115 (2017).
[2]Z. Yao, L. Nie, Y. Yue, Z. He, Y. Ke, Y. Mo, and H. Wang, "Network periodic train timetabling with integrated stop planning and passenger routing: A periodic time–space network construct and ADMM algorithm," Transp. Res. C: Emerg. Technol. **153**, 104201 (2023).
[3]X. Yu, Z. Chen, F. Liu, and H. Zhu, "How urban metro networks grow: From a complex network perspective," Tunn. Undergr. Space Technol. **131**, 104841 (2023).
[4]K. M. Mittal, M. Timme, and M. Schröder, "Efficient self-organization of informal public transport networks," Nat. Commun. **15**, 4910 (2024).
[5]Y. Hu, M. Xu, M. Tang, D. Han, and Y. Liu, "Efficient traffic-aware routing strategy on multilayer networks," Commun. Nonlinear Sci. Numer. Simul. **98**, 105758 (2021).
[6]O. Artime, M. Grassia, M. De Domenico, J. P. Gleeson, H. A. Makse, G. Mangioni, M. Perc, and F. Radicchi, "Robustness and resilience of complex networks," Nat. Rev. Phys. **6**, 114–131 (2024).
[7]R. Albert, H. Jeong, and A.-L. Barabási, "Error and attack tolerance of complex networks," Nature **406**, 378–382 (2000).
[8]R. Pastor-Satorras and A. Vespignani, "Epidemic spreading in scale-free networks," Phys. Rev. Lett. **86**, 3200 (2001).
[9]A.-L. Barabási, "Network science," Philos. Trans. R. Soc. A: Math. Phys. Eng. Sci. **371**, 20120375 (2013).
[10]A. Arenas, A. Díaz-Guilera, J. Kurths, Y. Moreno, and C. Zhou, "Synchronization in complex networks," Phys. Rep. **469**, 93–153 (2008).
[11]S. Boccaletti, V. Latora, Y. Moreno, M. Chavez, and D.-U. Hwang, "Complex networks: Structure and dynamics," Phys. Rep. **424**, 175–308 (2006).
[12]A. A. Ganin, E. Massaro, A. Gutfraind, N. Steen, J. M. Keisler, A. Kott, R. Mangoubi, and I. Linkov, "Operational resilience: Concepts, design and analysis," Sci. Rep. **6**, 1–12 (2016).
[13]Z. Xu and S. S. Chopra, "Interconnectedness enhances network resilience of multimodal public transportation systems for safe-to-fail urban mobility," Nat. Commun. **14**, 4291 (2023).
[14]V. K. Shante and S. Kirkpatrick, "An introduction to percolation theory," Adv. Phys. **20**, 325–357 (1971).
[15]A. A. Saberi, "Recent advances in percolation theory and its applications," Phys. Rep. **578**, 1–32 (2015).
[16]J. Xie, X. Wang, L. Feng, J.-H. Zhao, W. Liu, Y. Moreno, and Y. Hu, "Indirect influence in social networks as an induced percolation phenomenon," Proc. Natl. Acad. Sci. U.S.A. **119**, e2100151119 (2022).
[17]J. Qian, D. Han, and Y. Ma, "Criticality and continuity of explosive site percolation in random networks," Europhys. Lett. **100**, 48006 (2012).
[18]Z. Chen, C. Yang, J.-H. Qian, D. Han, and Y.-G. Ma, "Recursive traffic percolation on urban transportation systems," Chaos **33**, 033132 (2023).
[19]Y. Bao, "Research on the reliability and topological spatiotemporal evolution and simulation modeling of complex subway systems," Chinese graduate dissertation (Fudan University, 2024).
[20]L. Ambühl, M. Menendez, and M. C. González, "Understanding congestion propagation by combining percolation theory with the macroscopic fundamental diagram," Commun. Phys. **6**, 26 (2023).
[21]G. Zeng, J. Gao, L. Shekhtman, S. Guo, W. Lv, J. Wu, H. Liu, O. Levy, D. Li, Z. Gao *et al.*, "Multiple metastable network states in urban traffic," Proc. Natl. Acad. Sci. U.S.A. **117**, 17528–17534 (2020).
[22]F. Morone and H. A. Makse, "Influence maximization in complex networks through optimal percolation," Nature **524**, 65–68 (2015).
[23]H. Sun, F. Radicchi, J. Kurths, and G. Bianconi, "The dynamic nature of percolation on networks with triadic interactions," Nat. Commun. **14**, 1308 (2023).
[24]D. D. Woods, "Four concepts for resilience and the implications for the future of resilience engineering," Reliab. Eng. Syst. Safety **141**, 5–9 (2015).
[25]V. Gaur, O. P. Yadav, G. Soni, and A. P. S. Rathore, "A literature review on network reliability analysis and its engineering applications," Proc. Inst. Mech. Engr. O: J. Risk Reliab. **235**, 167–181 (2020).
[26]I. Linkov, T. Bridges, F. Creutzig, J. Decker, C. Fox-Lent, W. Kröger, J. H. Lambert, A. Levermann, B. Montreuil, J. Nathwani *et al.*, "Changing the resilience paradigm," Nat. Clim. Change **4**, 407–409 (2014).
[27]National Research Council, *Disaster Resilience: A National Imperative* (The National Academies Press, Washington, DC, 2012).
[28]D.-M. Zhang, F. Du, H. Huang, F. Zhang, B. M. Ayyub, and M. Beer, "Resiliency assessment of urban rail transit networks: Shanghai metro as an example," Safety Sci. **106**, 230–243 (2018).
[29]M. Jusup, P. Holme, K. Kanazawa, M. Takayasu, I. Romić, Z. Wang, S. Geček, T. Lipić, B. Podobnik, L. Wang *et al.*, "Social physics," Phys. Rep. **948**, 1–148 (2022).
[30]R. Massobrio and O. Cats, "Topological assessment of recoverability in public transport networks," Commun. Phys. **7**, 108 (2024).
[31]H. Hamedmoghadam, M. Jalili, H. L. Vu, and L. Stone, "Percolation of heterogeneous flows uncovers the bottlenecks of infrastructure networks," Nat. Commun. **12**, 1254 (2021).
[32]Z. Xu and S. S. Chopra, "Network-based assessment of metro infrastructure with a spatial–temporal resilience cycle framework," Reliab. Eng. Syst. Safety **223**, 108434 (2022).
[33]O. Lordan and J. M. Sallan, "Dynamic measures for transportation networks," PLoS One **15**, e0242875 (2020).
[34]D. Luo, O. Cats, H. van Lint, and G. Currie, "Integrating network science and public transport accessibility analysis for comparative assessment," J. Transp. Geogr. **80**, 102505 (2019).
[35]F. Ma, W. Shi, K. F. Yuen, Q. Sun, X. Xu, Y. Wang, and Z. Wang, "Exploring the robustness of public transportation for sustainable cities: A double-layered network perspective," J. Cleaner Prod. **265**, 121747 (2020).
[36]W. Zhu, K. Liu, M. Wang, and X. Yan, "Enhancing robustness of metro networks using strategic defense," Physica A **503**, 1081–1091 (2018).
[37]X.-B. Cao, C. Hong, W.-B. Du, and J. Zhang, "Improving the network robustness against cascading failures by adding links," Chaos Soliton. Fract. **57**, 35–40 (2013).
[38]X. Yao, B. Han, D. Yu *et al.*, "Simulation-based dynamic passenger flow assignment modelling for a schedule-based transit network," Discrete Dyn. Nat. Soc. **2017**(1), 2890814.
[39]U. Brandes, "A faster algorithm for betweenness centrality," J. Math. Soc. **25**, 163–177 (2001).
[40]H. Wang, J. M. Hernandez, and P. Van Mieghem, "Betweenness centrality in a weighted network," Phys. Rev. E **77**, 046105 (2008).

[41] Y. Yang, T. Nishikawa, and A. E. Motter, "Small vulnerable sets determine large network cascades in power grids," Science **358**, eaan3184 (2017).
[42] D. Li, B. Fu, Y. Wang, G. Lu, Y. Berezin, H. E. Stanley, and S. Havlin, "Percolation transition in dynamical traffic network with evolving critical bottlenecks," Proc. Natl. Acad. Sci. U.S.A. **112**, 669–672 (2015).
[43] H. Rakha and M. Van Aerde, "Statistical analysis of day-to-day variations in real-time traffic flow data," Transp. Res. Record **1995**, 26–34.
[44] M. Barthélemy, "Spatial networks," Phys. Rep. **499**, 1–101 (2011).
[45] S. Zanero, "Cyber-Physical Systems," Computer **50**(4), 14–16 (2017).
[46] O. Cats, "Topological evolution of a metropolitan rail transport network: The case of Stockholm," J. Transp. Geogr. **62**, 172–183 (2017).
[47] J. Zhang, W. Klingsch, A. Schadschneider, and A. Seyfried, "Transitions in pedestrian fundamental diagrams of straight corridors and T-junctions," J. Stat. Mech.: Theory Exp. **2011**, P06004 (2011).